The Journal of Neuroscience, January 15, 2000, *20*(2):820–833

Relationship of Activity in the Subthalamic Nucleus–Globus Pallidus Network to Cortical Electroencephalogram

Peter J. Magill, J. Paul Bolam, and Mark D. Bevan

Medical Research Council Anatomical Neuropharmacology Unit, University Department of Pharmacology, Oxford, OX1 3TH, United Kingdom

One of the functions of the excitatory subthalamic nucleus (STN) is to relay cortical activity to other basal ganglia structures. The response of the STN to cortical input is shaped by inhibition from the reciprocally connected globus pallidus (GP). To examine the activity in the STN–GP network in relation to cortical activity, we recorded single and multiple unit activity in STN and/or GP together with cortical electroencephalogram in anesthetized rats during various states of cortical activation.

During cortical slow-wave activity (SWA), STN and GP neurons fired bursts of action potentials at frequencies that were similar to those of coincident slow (~1 Hz) and spindle (7–14 Hz) cortical oscillations. Spontaneous or sensory-driven global activation was associated with a reduction of SWA and a shift in STN–GP activity from burst- to tonic- or irregular-firing. Rhythmic activity in STN and GP neurons was lost when the cortex was inactivated by spreading depression and did not resume until SWA had recovered.

Although rhythmic STN–GP activity was correlated with SWA, the phase relationships of activities of neurons within the STN and GP and between the nuclei were variable. Even when neurons displayed synchronous bursting activity, correlations on the millisecond time scale, which might indicate shared synaptic input, were not observed.

These data indicate that (1) STN and GP activity is intimately related to cortical activity and hence the sleep–wake cycle; (2) rhythmic oscillatory activity in the STN–GP network in disease states may be driven by the cortex; and (3) activity of the STN–GP network is regulated in space in a complex manner.

Key words: subthalamic nucleus; globus pallidus; basal ganglia; cortex; EEG; slow-wave; spindle; oscillation; activation; sleep; Parkinson's disease

The glutamatergic subthalamic nucleus (STN) is a key integrative structure in the circuitry of the basal ganglia (Alexander and Crutcher, 1990; Smith et al., 1998). It receives and relays excitatory signals from the cortex and thalamus to basal ganglia output nuclei (Rouzaire-Dubois and Scarnati, 1987; Canteras et al., 1990; Nambu et al., 1990; Robledo and Féger, 1990; Fujimoto and Kita, 1992, 1993; Ryan and Sanders, 1993, 1994; Mouroux et al., 1995; Maurice et al., 1999). GABAergic neurons of the globus pallidus (GP) shape the response of STN neurons and their targets to cortical stimulation by two mechanisms. First, by feedback inhibition via their reciprocal connections with the STN (Rouzaire-Dubois et al., 1980; Kita et al., 1983b; Smith et al., 1990; Ryan and Clark, 1991; Fujimoto and Kita, 1993; Bevan et al., 1995, 1997; Maurice et al., 1998a,b) and second, by a disinhibitory mechanism involving corticostriatal and striatopallidal pathways (Ryan and Clark, 1991; Ryan et al., 1992; Ryan and Sanders, 1994; Maurice et al., 1998a; Smith et al., 1998). Thus, the complex spatiotemporal patterns of facilitation and inhibition of basal ganglia structures that follow cortical excitation during movement are likely to be supported, in part, by the STN–GP network (Nambu et al., 1990). The functional properties of this network, in turn, are likely to be dependent on cortical activity (Aldridge et al., 1990; Aldridge and Gilman, 1991).

The responses of the STN and GP to brief cortical stimulation have been described in detail (Kitai and Deniau, 1981; Rouzaire-Dubois and Scarnati, 1985; Nambu et al., 1990; Ryan and Clark, 1991; Kita, 1992; Fujimoto and Kita, 1993; Yoshida et al., 1993; Maurice et al., 1998a), but the activity of the STN–GP network in relation to natural patterns of cortical activity remains to be established. To test the hypothesis that the activity of the STN–GP network is dependent on the pattern of cortical input, we studied network behavior during various states of cortical activation. In natural slow-wave sleep and anesthesia, cortical activity is characterized by regularly alternating periods of synchronous spike discharge and neuronal silence in projection neurons (Evarts, 1964; Armstrong-James and Fox, 1983; Buzsáki et al., 1988; Steriade et al., 1993c,d; Stern et al., 1997; Steriade and Amzica, 1998; Destexhe et al., 1999). Furthermore, brief periods of cortical activation that occur because of capricious fluctuations in slow-wave activity (SWA), or that result from sensory stimulation, are analogous to global arousal (Buzsáki et al., 1988; Steriade et al., 1990, 1993a; Metherate et al., 1992; Contreras and Steriade, 1997b). Thus, the anesthetized preparation is a good model for establishing the impact of extremes of cortical activity on the STN–GP network. We therefore recorded spike discharge of single and paired STN and GP neurons and coincident cortical electroencephalogram (EEG) during various stereotyped modes of cortical activity.

Received Aug. 19, 1999; revised Oct. 11, 1999; accepted Oct. 29, 1999.

This work was supported by the Medical Research Council UK and the Wellcome Trust (Advanced Training Fellowship 046613/Z/96/Z) (M.D.B.). P.J.M. is in receipt of a Medical Research Council studentship. We gratefully acknowledge Dr. Y. Kaneoke for the provision and modification of the burst and oscillation detection algorithms and Dr. E. A. Stern for the correlation analysis routines. We thank Drs. C. J. Wilson and G. W. Arbuthnott for their invaluable comments and discussions, and Liz Norman and Caroline Francis for technical assistance.

Correspondence should be addressed to Dr. Mark D. Bevan, Medical Research Council Anatomical Neuropharmacology Unit, Mansfield Road, Oxford, OX1 3TH, UK. E-mail: mark.bevan@pharm.ox.ac.uk.

Copyright © 2000 Society for Neuroscience 0270-6474/00/200820-14$15.00/0

The discharge of STN and GP neurons within and between connected regions of the parent nuclei during wakefulness displays little or no correlation (Bergman and DeLong, 1989; Wichmann et al., 1994; Bergman et al., 1998) (H. Kita, personal communication). Uncorrelated activity in the STN–GP network might arise from asynchronous afferent input or may result from a pattern of hardwiring that ensures that individual neurons receive few common inputs (Bergman and DeLong, 1989; Bevan et al., 1997). These hypotheses were tested by intra- and internuclear STN and GP recordings during periods of synchronous cortical input that were associated with SWA. A low incidence of correlated discharge during the synchronous cortical activity present in sleep and anesthesia would favor the hypothesis that uncorrelated activity within the STN–GP network is attributable to a low degree of input sharing.

Subthalamic and GP neuronal discharge changes from asynchronous and irregular firing in health to a pattern of synchronous, rhythmic burst-firing in idiopathic or animal models of Parkinson's disease (PD) (Filion and Tremblay, 1991; Bergman et al., 1994; Wichmann et al., 1994; Nini et al., 1995; Hassani et al., 1996; Kreiss et al., 1997; Boraud et al., 1998). This rhythmic activity is phase-related to resting tremor in PD (Bergman et al., 1994, 1998). Recent investigations of organotypic cocultures suggest that the STN–GP network alone can support this pattern of activity and act as a generator of resting tremor (Plenz et al., 1997). To determine whether the STN–GP network in isolation from the cortex can support synchronous low-frequency oscillatory activity *in vivo*, cortical input was transiently suppressed using a spreading depression paradigm (Leão, 1944; Albe-Fessard et al., 1983; Contreras et al., 1997).

MATERIALS AND METHODS

Electrophysiological recording and labeling of neurons. Procedures involving animals were conducted in accordance with the Animals (Scientific Procedures) Act, 1986 (UK), and with the Society for Neuroscience policy on the use of animals in research. Experiments were performed on male Sprague Dawley rats (180–280 gm; Charles River, Margate, UK). Anesthesia was induced with isoflurane (Isoflo, Schering-Plough, Welwyn Garden City, UK) and maintained using one of the following two regimens: (1) ketamine (100 mg/kg, i.p.; Ketaset, Willows Francis, Crawley, UK) and xylazine (10 mg/kg, i.p.; Rompun, Bayer, Germany) plus supplemental doses as necessary, or (2) urethane (1.25 g/kg, i.p.; ethyl carbamate, Sigma, Poole, UK) plus supplemental doses of ketamine and xylazine (30 mg/kg and 3 mg/kg, i.p., respectively). Hereafter, group 1 shall be referred to as "ketamine"-anesthetized and group 2 shall be referred to as "urethane"-anesthetized. All pressure points and wound margins were infiltrated with lignocaine (2% with adrenalin, C-Vet, Leyland, UK), and corneal drying was prevented with frequent application of Hypromellose eye drops (Norton Pharmaceuticals, Harlow, UK). Animals were then placed in a stereotaxic frame (David Kopf Instruments, Tujunga, CA), and body temperature was maintained at 37 ± 0.5°C with the use of a homeothermic heating device (Harvard Apparatus, Edenbridge, UK). Anesthesia levels were assessed by examination of the EEG and by testing reflexes to a strong cutaneous pinch and gentle corneal stimulation. Electrocardiographic activity and respiration rate were also constantly monitored to ensure the animals' well-being. Small craniotomies were performed directly above the STN and/or GP, and the overlying dura mater was carefully removed. Mineral oil or saline solution (0.9% NaCl w/v) was applied to all areas of exposed cortex to prevent dehydration.

Extracellular recordings of action potentials of basal ganglia neurons were made with 15–25 MΩ glass electrodes (tip diameter ~1.5 μm) filled with a 0.5 M NaCl solution containing 1.5% neurobiotin (Vector, Peterborough, UK). Electrode signals were amplified (10 times) through the active bridge circuitry of an Axoprobe-1A amplifier (Axon Instruments, Foster City, CA), AC-coupled, and amplified a further 100 times (AC-DC Amp, Digitimer, Welwyn Garden City, UK) before being filtered between 0.3 and 5 kHz (NL125, Digitimer). Last, signals were collected on tape (60ES DAT system, Sony, UK) and displayed simultaneously on a digital oscilloscope (DSO 610, Gould Instruments, Ilford, Essex, UK). This protocol was used to perform single or double recordings of neurons. Spikes were often several millivolts in amplitude and always exhibited a biphasic waveform with an initial positive deflection. Recordings of spontaneous activity typically lasted for 4–25 min. The EEG was recorded via a steel screw juxtaposed to the dura mater above the ipsilateral or contralateral frontal cortex (2.7 mm anterior to bregma and 2.0 mm lateral to the midline, according to the atlas of Paxinos and Watson, 1986) and referenced against an indifferent electrode placed adjacent to the temporal musculature. Raw EEG was bandpass-filtered (0.1–100 Hz) and amplified (2000 times) with a NL104 preamplifier (Digitimer), collected on tape with concurrent spiking activity, and displayed on the same oscilloscope. Cortical spreading depression was elicited by the topical application of a 3 M potassium acetate solution unilaterally to the surface of the frontal cortex that was ipsilateral to the recording site. Sensory stimulation was elicited by pinching the hindpaw at the level of the palm/plantar using pneumatically driven serrated forceps. The forceps exerted a standard pressure when closed. For multiple recordings, a long interstimulus interval (>15 min) was used to allow recovery of responses. To identify the location of recorded units, neurons were then selectively labeled with neurobiotin by the juxtacellular method (Pinault, 1996; Bevan et al., 1998). Briefly, the electrode was slowly advanced toward the neuron while a low-intensity microiontophoretic current was applied (1–10 nA anodal current, 200 msec duration, 50% duty cycle). Optimal positioning was identified when the firing pattern of the neuron was robustly modulated during the current ejection. Generally, neuronal firing was modulated by the microiontophoretic current for at least 10 min to obtain reliable labeling. On five occasions (two STN and three GP neurons) when robust modulation could not be achieved, the position of the recorded unit was marked by a discrete extracellular deposit of neurobiotin (100 nA anodal current; 1 sec (50%) duty cycle for 30–60 min). After the experiment, the animals were given a lethal dose of anesthetic and perfused via the ascending aorta with 100 ml of 0.1 M PBS, pH 7.4, followed by 300 ml of 0.3% glutaraldehyde and 3% paraformaldehyde in 0.1 M phosphate buffer, pH 7.4, and then by 150 ml of the same solution without glutaraldehyde. Brains were then post-fixed in the latter solution at 4°C for at least 12 hr.

Histochemistry. Standard histochemical techniques were used to visualize the neurobiotin-filled cells (Horikawa and Armstrong 1988, 1991; Bevan et al., 1998). Briefly, the fixed brain was sectioned (50–60 μm) in the sagittal plane on a vibrating microtome. Sections were then washed in PBS and incubated in avidin–biotin peroxidase complex (1:100; Vector) in PBS containing 0.3% Triton X-100 overnight at room temperature. After washes, the slices were incubated in hydrogen peroxide (0.002% w/v; Sigma) and diaminobenzidine tetrahydrochloride (0.025% w/v; Sigma) in the presence of nickel ammonium sulfate (0.5% w/v; Sigma) for 15–30 min at room temperature. Neurobiotin-filled cells were intensely labeled with an insoluble, black/blue precipitate. Last, sections were dehydrated, cleared, and mounted for light microscopy as described previously (Bolam, 1992).

Data analysis. Unit activity and EEGs were sampled at 12 kHz and 200 Hz, respectively, and digitized off-line with the Spike 2 acquisition and analysis software (Cambridge Electronic Design, Cambridge, UK). Data from the entire recording session were visually inspected, and epochs of robust cortical slow-wave activity were identified. A portion of the coincident spike train composed of 100 spikes was then isolated and used in the statistical analysis of the spike-firing pattern. A modified version of the burst and oscillation detection algorithm of Kaneoke and Vitek (1996) was used to objectively and quantitatively determine the firing pattern and potential periodicity in these spike trains. Neurons were assigned a burst index (BI) according to the deviation of the distribution of spikes in the train from an irregular (Poisson) distribution. The more "bursty" a cell was, the greater its BI (Kaneoke and Vitek, 1996). A cell was defined as bursty when the BI was ≥0.5 and the spike train contained "bursts" (a burst was defined as a period that contained three or more spikes and the number of spikes was significantly greater than in other periods in the spike train). "Regular" (tonic) neurons fired no bursts, had a BI <0.1, and a (quasi) normally distributed first-order interval histogram. "Irregular" neurons were defined as cells that could not fit the strict criteria for either bursty or regular firing cells, i.e., they did not fire bursts and had a BI <0.5 and a slightly skewed interval histogram. The Lomb algorithm was used to determine the statistical significance and frequency of any periodic discharge features present in the spike train within the 0.5–50 Hz range (Kaneoke and Vitek, 1996; Boraud et al.,

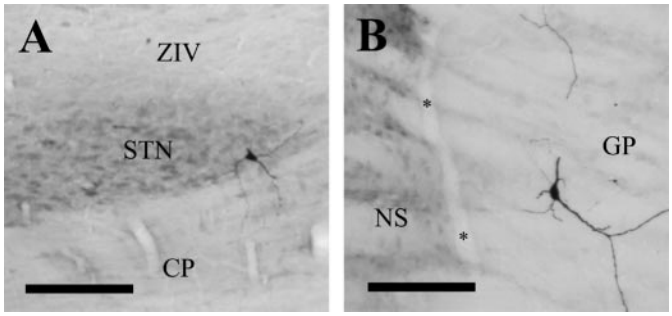

Figure 1. Light micrographs of subthalamic nucleus and globus pallidus neurons that were juxtacellularly labeled with neurobiotin. *A*, This STN neuron was located in the caudal portion of the more darkly stained STN. *ZIV*, Ventral division of the zona incerta; *CP*, cerebral peduncle. *B*, This GP neuron was situated in the rostral aspect of the GP. A blood vessel (*) lies on the border between the GP and the more darkly stained neostriatum (*NS*). Rostral is to the *left*, and dorsal is to the *top* of each figure. Scale bars, 200 μm.

1998; Ruskin et al., 1999). Frequency spectra of spiking are displayed as "Lomb periodograms." The relative power of a peak in the periodogram is indicated by the clearance of the peak from the significance level of $p = 0.05$ (represented by *dashed line* in Figs. 2 -8, inclusive).

Auto- and cross-correlograms of action potentials were calculated for the same 100 spikes of data using Mathematica routines (Wolfram Research, Long Hanborough, UK) based on standard methods and a bin size of 1, 5, or 10 msec (Perkel et al., 1967; Abeles, 1982; Stern et al., 1998). To facilitate the approximation of phase lags, correlograms were smoothed using a three-point moving average of the raw data. Spike-triggered waveform averages across these samples were performed with Spike 2 and used to estimate phase relationships between the EEG and spike-firing. Mean firing frequency was calculated from the reciprocal of the mean interspike interval. Power spectra of the EEG were calculated from the waveform data overlapping the sampled spike train using the Fast Fourier Transform function of Spike 2. Statistical comparisons of firing rates and oscillation frequencies were conducted using the Mann–Whitney *U* test. The Wilcoxon signed rank test was used in the determination of significance for paired data (e.g., pinch effects). The criterion for significance for all tests was taken to be at least 95%. All data are expressed as mean ± SD. The precise locations of all recorded neurons were verified under the light microscope.

RESULTS

Juxtacellularly labeled STN and GP neurons

After physiological characterization of single or multiple units, robust modulation of the firing of a single unit with microiontophoresis always led to a single neuron being well labeled (Fig. 1). Subthalamic nucleus neurons were situated throughout the nucleus (Fig. 1*A*). In contrast, most of the GP neurons were located in the medial half of GP (Fig. 1*B*).

Characterization of EEG activity

Regardless of anesthetic protocol, surgical anesthesia was accompanied by regularly occurring slow-waves of large amplitude (>500 μV) in the frontal EEG (Figs. 2, 3). Slow-wave activity in the ketamine-anesthetized group had a significantly faster frequency of oscillation than that recorded in animals under urethane anesthesia (Tables 1, 2). Higher-frequency activity, which was of a smaller amplitude (<200 μV), was commonly superimposed on specific portions of the large slow-waves (Fig. 2*B,C*). These portions of the slow oscillation are associated with synchronous spike discharge in cortical projection neurons (Steriade and Amzica, 1998) and will be referred to as the "active components." The frequency range of the smaller amplitude waves varied widely, but spindle activity in the 7–14 Hz range was often predominant (Steriade et al., 1990, 1993d; McCormick and Bal, 1997; Amzica and Steriade, 1998; Steriade and Amzica, 1998).

Physiological characteristics of STN neurons

Extracellular unit recordings revealed that STN neurons exhibited both bursty and irregular firing patterns at variable firing rates under both anesthetic regimens (Table 1). However, the mean spontaneous firing rate of STN neurons recorded under ketamine was significantly higher than the mean rate of neurons recorded under urethane (Table 1) ($p < 0.01$). In addition, STN neurons were proportionally more bursty in ketamine-based than in urethane-based anesthesia (84 and 60% of each cell population maintained a BI ≥1.0, respectively).

During episodes of robust SWA, the rhythmic cortical oscillation was mirrored in the spontaneous firing patterns of STN neurons (Figs. 2*A,B*, 3*A*) ($n = 29$). Indeed, burst firing of STN neurons was correspondingly periodic (see autocorrelograms in Figs. 2*A,B*, 3*A*) and was precisely phase-locked with SWA (see spike-triggered waveform averages in Figs. 2*A,B*, 3*A*). Spike firing of STN neurons was always restricted to the active component of the slow oscillation (Fig. 2*B*). In addition, STN bursts could be subdivided into "miniature bursts" (one to four spikes) that were phase-locked to the spindle sequences superimposed on the SWA (Fig. 2*B,C*). A statistical comparison of Lomb periodograms, which are measures of significant oscillations in the spike train, with the power spectra of the EEG demonstrated a similar periodicity (Fig. 2*A,B*, Table 1).

Spontaneous, short-lived losses of EEG power (i.e., rhythmicity and amplitude) in the slow-wave and spindle frequency range, a process hereafter referred to as "activation," were always reflected as changes in firing patterns of STN neurons. They rapidly adopted an irregular, single-spike firing pattern during episodes of activated cortical patterns (Figs. 2*A,* 3*B*, 5*B,C*). Activation mechanisms originating in the brain stem and/or forebrain can be recruited by sensory input from the periphery to activate the cortex and obliterate SWA in the EEG (Moruzzi and Magoun, 1949; Détári and Vanderwolf, 1987; Buzsáki et al., 1988; Steriade et al., 1990, 1993a; Nuñez, 1996). Hindpaw pinching was rarely effective in fully activating the frontal EEG in animals anesthetized with ketamine [see also Svoboda et al. (1999)]. However, a small decrease in SWA amplitude and periodicity was observed in 9 of 14 cases. This was closely linked with a significant decrease in firing rate of STN neurons (54.7 ± 18.2% of spontaneous levels) but was usually not associated with a change in gross firing pattern. Under urethane anesthesia, somatosensory responses are left relatively intact (Angel and Gratton, 1982; Maggi and Melli, 1986; Nuñez, 1996), and indeed we found that paw pinch was more effective in activating the frontal cortex in urethane-anesthetized animals. Activation of the EEG was commensurate with a loss of bursting and a change in firing to an irregular, single-spike pattern, together with a significant increase in firing rate (136.6 ± 43.0% of control; $n = 5$) (Figs. 3*,* 7*B*). It should be noted, however, that a profound change in firing pattern can occur with a relatively minor change in firing rate (Fig. 3; pinch caused firing rate to increase to only 110.9% of control, but bursting was completely lost). Fluctuations in firing rate and firing pattern of STN neurons in response to pinch were only observed when changes in cortical activity occurred. Taken together, these findings suggest that there is a tight relationship between cortical activity and somatosensory responses in the STN during both types of anesthesia.

The relationship between cortical and STN activity was further

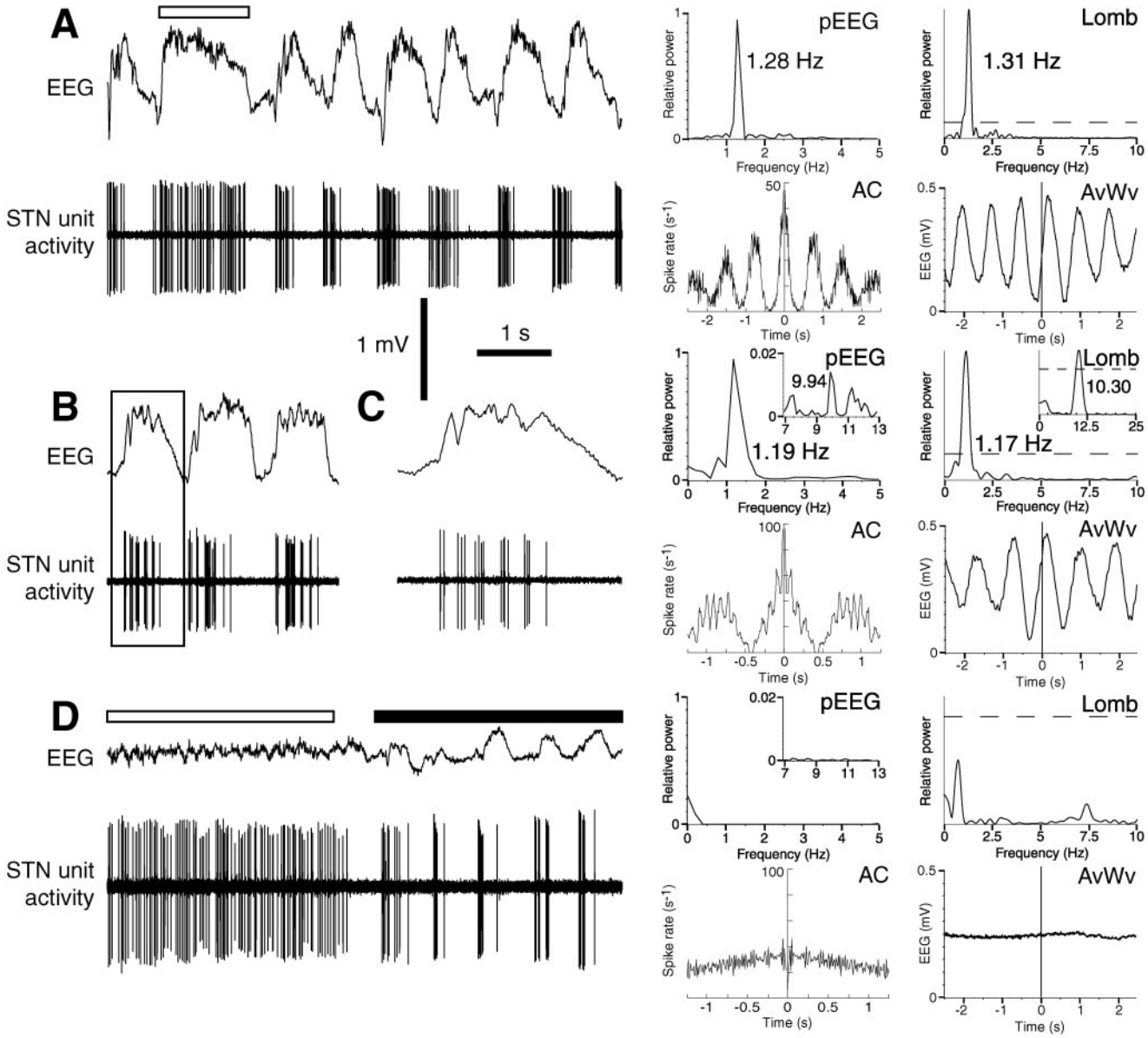

Figure 2. Spike-firing patterns of subthalamic nucleus neurons are related to coincident cortical activity during ketamine anesthesia. *A*, This STN neuron had a BI of 1.43 and fired robust bursts of spikes on the rising phase of the slow cortical oscillation. Note that during periods of prolonged cortical activation (under *white bar*), the burst duration was increased. Rhythmic spike-firing was manifest as peaks in the autocorrelogram (*AC*). Comparison of the Lomb periodogram (*Lomb*) with the power spectrum of the EEG (*pEEG*) shows a similar frequency of rhythmic activity in the STN spike train and cortex. *Dashed line* in this and subsequent Lomb periodograms denotes the significance level of $p = 0.05$. The phase relationship between spiking and the EEG waves is shown on the spike-triggered waveform average (*AvWv*). *B*, The firing of another bursty neuron (BI = 1.0) was phase-locked to the crest of the cortical slow-wave. Note the smaller amplitude, spindle-like events (frequency ~10 Hz) superimposed on the peaks of the slow-wave in the EEG trace. The large bursts occurred at a frequency of ~1 Hz and were composed of a number of "miniature bursts," which are shown as small peaks riding on the top of the three larger peaks in the autocorrelogram. The main Lomb periodogram shows significant bursting at a frequency very similar to that of the large slow-wave. The *inset* Lomb is filtered between 4 and 25 Hz and shows a significant oscillation in the spike train at ~10 Hz frequency. *C*, The *boxed area* in *B* (1 sec of data) on an expanded time scale. The firing of miniature bursts was phase-locked with the generation of the spindle-like wavelets. *D*, Burst activity in the same neuron was replaced with irregular, single-spike activity during episodes of cortical spreading depression (*white bar*). The four graphs to the *right* of the trace in *D* were constructed from the period under the *white bar*; note that a significant oscillation in the Lomb was no longer present and that the autocorrelogram did not have peaks when power in the EEG was severely attenuated. Partial recovery of cortical SWA was accompanied by a partial restoration of burst activity (*black bar*). Calibration bars apply to all panels except *C*. In this and the following figures, *AC* designates autocorrelograms of spiking activity (bin size 10 msec), *Lomb* designates Lomb periodograms of spiking activity, *pEEG* designates power spectra of the coincident EEG, and *AvWv* designates spike-triggered averages of EEG.

analyzed by testing neuronal responses to transient cortical inactivation induced by spreading depression (Leão, 1944; Albe-Fessard et al., 1983; Contreras et al., 1997). This resulted in a graded loss of coherent, rhythmic activity in the cortex (SWA reduced to 5–25% of original power) (Fig. 2*D*), which was associated with a loss of bursting, a change to irregular firing, and a significant drop in spike rate in the ipsilateral STN (28.4 ± 26.2% of control; one neuron became quiescent; $n = 5$). Although the effects of the depression on firing rate were highly variable, this switch in firing mode was robust. In most cases the depression of

Table 1. Spike-firing properties of subthalamic nucleus neurons

	Type of anesthesia	
	Urethane	Ketamine
Total number of cells	10	19
Firing rate (Hz)	10.6 ± 6.2	21.2 ± 11.4
Number of bursty cells[a]	9	18
Number of irregular cells	1	1
Number of regular cells	0	0
Number of oscillating cells[b]	10	19
Frequency of spike train oscillation (Hz)	0.75 ± 0.33	1.33 ± 0.19
Frequency of cortical SWA (Hz)	0.81 ± 0.15	1.34 ± 0.19

Data are expressed as mean ± SD.

[a]Bursty cells had a BI ≥0.5.

[b]Oscillating cells were defined as displaying a significant oscillation in their spike trains ($p < 0.05$).

cortical activity was fully reversible, and bursting activity only resumed when SWA reappeared (Fig. 2*D*). These data suggest that the cortex directly or indirectly exerts an excitatory influence on the neurons of the STN and that oscillatory activity in the STN is not maintained in the absence of rhythmic cortical input.

Physiological characteristics of GP neurons

Similar to the observations in the STN under ketamine anesthesia, GP neurons exhibited both bursty and irregular firing patterns at variable firing rates (Table 2). In contrast, under urethane anesthesia, GP neurons discharged single spikes in a regular manner even when SWA simultaneously occurred in the cortex (Fig. 4*C*) ($n = 15$). Furthermore, GP neurons recorded during urethane anesthesia were significantly more active than those recorded in ketamine anesthesia.

Cortical oscillations were reflected in the spontaneous firing patterns of the majority of GP neurons recorded under ketamine anesthesia. Indeed, 91% of GP neurons recorded ($n = 32$) expressed a significant oscillation in their spike train with a frequency that was similar to the concurrent slow oscillation in the frontal cortex (Table 2). Most of the oscillating GP cells were irregular (59%), with the remaining 41% being bursty (Table 2) (firing rates not significantly different). In contrast to STN neurons, GP neurons fired spikes during either the active or inactive components of the slow oscillation (Figs. 4*A*, 8*A*). The large burst discharges of pallidal neurons were occasionally divided into miniature bursts in time with the coincident spindles (Figs. 4*A*, 5*A*).

Spontaneous or pinch-evoked activation of cortex in ketamine anesthesia typically resulted in a loss of bursting activity of GP neurons with either a decrease (65.7 ± 18.1% of control; 8 of 30 neurons tested) or an increase (231.2 ± 116.0% of control; 6 of 30 neurons) in firing (Figs. 5*B*,*C*, 8*C*). In 10 cases, the pinch caused no change in the EEG or spike discharge. Cortical inactivation by spreading depression resulted in a decrease in SWA and a profound reduction in spike-firing rate (26.8 ± 35.7% of predepression spike rates; $p < 0.05$; $n = 5$) (Fig. 4*B*). In three neurons, cortical inactivation resulted in total quiescence, which persisted for the duration of the spreading depression. These data suggest that the cortex indirectly or directly exerts an excitatory influence on the neurons of the GP and that oscillatory activity in the GP is not maintained in the absence of rhythmic cortical activity.

A neuron with a regular discharge pattern will have a significant peak in the Lomb periodogram that is similar to the mean rate of spiking. The highly regular nature of firing in the GP under urethane was demonstrated by the fact that these two values did not differ significantly for GP neurons (Fig. 4*C* and Table 2). Neuronal firing rate and pattern were relatively insensitive to minor fluctuations in SWA. However, the hindpaw pinch, which typically caused a robust activation of the EEG, was associated with a significant increase in firing rate (136.0 ± 30.5%; $n = 7$). In one case, the paw pinch failed to activate the cortex or change the firing rate of the GP neuron. As was the case for STN neurons, fluctuations in firing rate and pattern of GP neurons after the pinch, under either anesthetic regime, were only observed when there were changes in cortical SWA. These data suggest that the cortex plays a fundamental role in mediating the responses of GP neurons to innocuous and painful tactile stimuli.

Simultaneously recorded STN and GP neurons

All seven pairs of neurons recorded simultaneously in ketamine anesthesia discharged spikes in a highly correlated manner that was phase-locked to the coincident cortical SWA (Fig. 5*A*). Correlated firing occurred on the time scale of tens and hundreds of milliseconds (see broad peaks of cross-correlogram in Fig. 5*A*), possibly reflecting input synchrony (Perkel et al., 1967). Correlations on the low millisecond time scale were not observed. The cross-correlation procedure was replicated for different epochs along the spike train, and phase relationships did not vary significantly when robust SWA was present. All seven STN neurons and five of seven GP neurons were bursty, but all 14 neurons displayed a significant oscillation in their spike trains. The mean frequency of this oscillation (1.41 ± 0.24 Hz) was not statistically different from the mean slow-wave oscillation in the EEG (1.39 ± 0.24 Hz). Oscillations in the spike trains of simultaneously recorded neurons were tightly coupled (mean disparity of 0.07 ± 0.08 Hz for the seven pairs). However, the phase relationships between the firing of STN and GP neurons varied between 5 and 330 msec (~2–135° phase shift). It cannot be ascertained from the present study whether the pairs of neurons were recorded from functionally equivalent and/or reciprocally connected areas of the STN and GP. Thus, these data imply that although the temporal aspects of oscillatory activity in the STN–GP network are strictly related to cortical activity, the phase differences in firing may be determined by the spatial constraints of the network.

Correlated firing of STN and GP neurons was transiently lost during capricious, or experimentally evoked, fluctuations in SWA (Fig. 5*B*; also compare cross-correlograms in Fig. 5*A*,*C*). Indeed, episodes of cortical activation were immediately accompanied by a switch from correlated bursting to uncorrelated irregular firing patterns in both types of neuron (Figs. 5*B*,*C*). Taken together with the results from singularly recorded cells, these data suggest that correlated bursting at 0.5–2 Hz is unlikely to be generated within the STN–GP network itself and is most probably not a self-perpetuating oscillation in the absence of rhythmic cortical input.

Seven pairs of STN and GP neurons recorded simultaneously in urethane did not exhibit any correlation in spike-firing (Fig. 6). The lack of synchrony between the two nuclei was manifest as regular-firing in GP neurons concomitant with bursting in STN neurons that was phase-locked to cortical SWA. Uncoordinated activity in the STN–GP network was not caused by atypical SWA because there was no significant difference in the amplitude and frequency of the SWA in the paired- or single-neuron recording sessions.

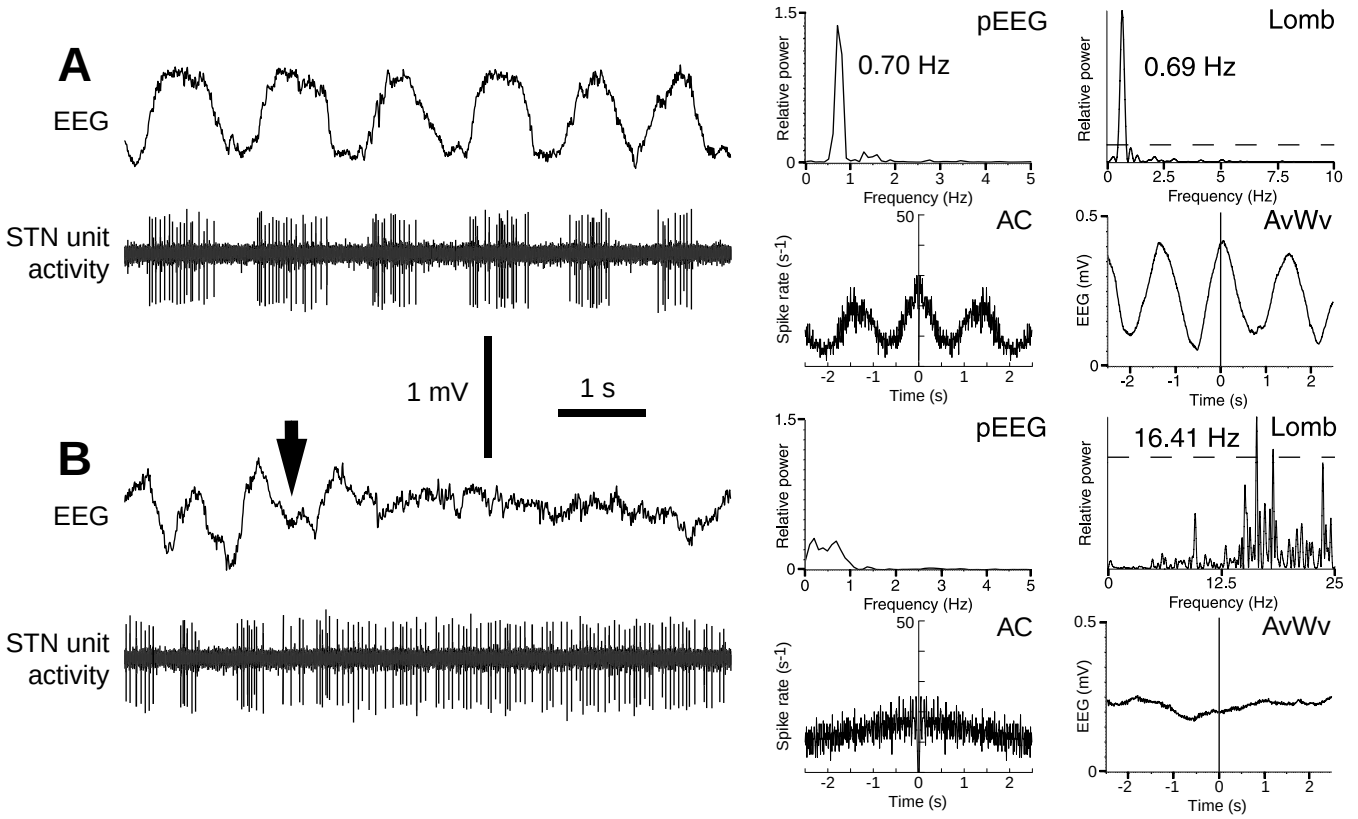

Figure 3. Spike-firing patterns of subthalamic nucleus neurons are related to coincident cortical activity in urethane anesthesia. *A*, A bursty STN neuron (BI = 0.67), the firing of which was phase-locked to SWA. Note the significantly lower frequency of SWA and periodic bursting as compared with activity during ketamine anesthesia. *B*, Disruption of SWA by sensory stimulation (hindpaw pinch of 10 sec duration; starts at *black arrow*) was concomitant with a loss of bursty activity in the same neuron. AC, Lomb, pEEG, and AvWv in *B* were determined during the pinch. Calibration bars apply to both panels.

Table 2. Spike-firing properties of globus pallidus neurons

	Type of anesthesia	
	Urethane	Ketamine
Total number of cells	15	32
Firing rate (Hz)	21.7 ± 7.9	13.1 ± 7.4
Number of bursty cells[a]	0	13
Number of irregular cells	0	19
Number of regular cells	15	0
Number of oscillating cells[b]	15	29
Frequency of spike train oscillation (Hz)	24.54 ± 7.60	1.26 ± 0.25
Frequency of cortical SWA (Hz)	0.83 ± 0.15	1.24 ± 0.22

Data are expressed as mean ± SD.

[a]Bursty cells had a BI ≥0.5.

[b]Oscillating cells were defined as displaying a significant oscillation in their spike trains ($p < 0.05$).

Simultaneously recorded pairs of STN neurons

The variation in phase relationships between burst-firing STN and GP neurons recorded simultaneously may be attributable, in part, to asynchronous firing within the STN and/or GP. To determine this, multiunit recordings from single electrodes were made in the STN under ketamine and urethane anesthesia. In good agreement with single-unit recordings, spike-firing in pairs of neurons was phase-locked to cortical activity (Fig. 7). The oscillation in the spike trains of four pairs of STN neurons (1.25 ± 0.14 Hz) was not significantly different from that of the slow cortical oscillation (1.29 ± 0.18 Hz) during ketamine anesthesia. Furthermore, the discharge of neighboring STN cells was tightly correlated and occurred only during the active component of the SWA (Fig. 7*A*), which resulted in a small difference in the frequency of oscillatory firing between paired neurons (mean difference of 0.10 ± 0.03 Hz). However, the phase relationships of firing in pairs were inconsistent, falling in the range of 5–65 msec (~1–13° phase shift). Broad, symmetrical peaks spanning hundreds of milliseconds in the cross-correlograms of neighboring STN neurons suggests that correlated firing is a possible consequence of input synchrony (Fig. 7*A,B*) [see also Ryan et al. (1992) and Wichmann et al. (1994)]. Correlated firing on the low millisecond time scale was not observed. A loss of SWA was associated with a suppression of correlated firing (Fig. 7*B*). These results suggest that local synchrony in the STN is directly or indirectly dependent on synchronous rhythmic input descending from the cortex to the basal ganglia.

Simultaneously recorded pairs of GP neurons

To elucidate the potential contribution of the GP to the varied phase relationships seen in the STN–GP network, single-cell recordings were made from pairs of electrodes in the GP during ketamine anesthesia. In good agreement with single-unit recordings, spike discharge was intimately related to the coincident SWA (Fig. 8). Indeed, the frequencies of the slow oscillation present in the spike trains of six pairs of GP neurons (1.23 ± 0.19 Hz) and the cortex (1.19 ± 0.14 Hz) were very similar. The oscillatory discharge of pairs of GP cells was tightly coupled

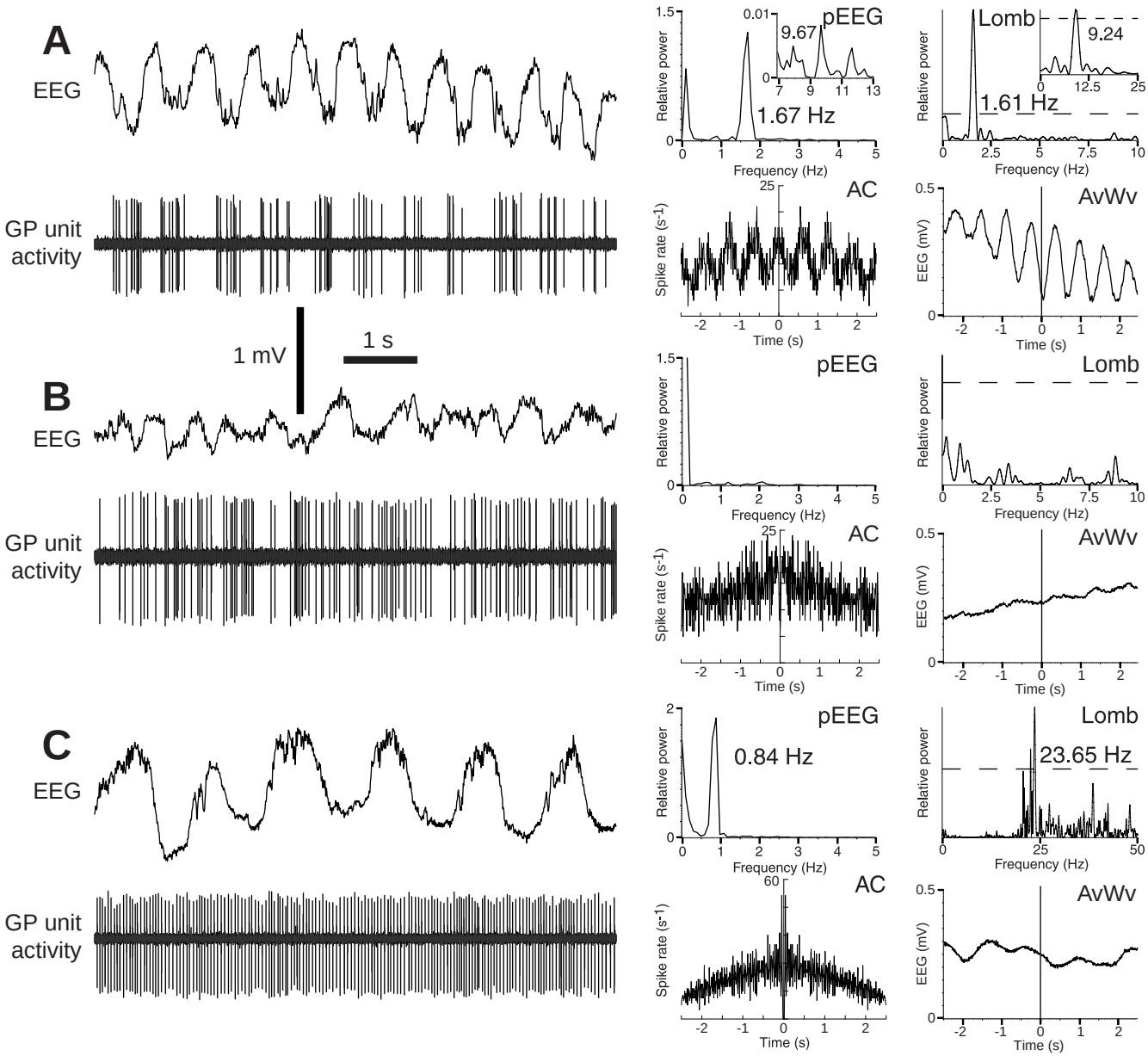

Figure 4. Spike-firing patterns of globus pallidus neurons are related to coincident cortical activity. *A*, A bursty, pallidostriatal GP neuron (BI = 0.67) firing well defined bursts of spikes during the troughs of the slow-wave during ketamine anesthesia. Comparison of the Lomb with the power spectrum shows very similar frequencies of rhythmic activity in the spike train and EEG. The main Lomb periodogram shows significant bursting at a frequency very similar to that of the large slow-wave; the *inset* Lomb is filtered between 4 and 25 Hz and shows a significant oscillation in the spike train at ~10 Hz frequency, which is similar to the spindle frequency. *B*, During cortical spreading depression, the amplitude of the SWA was attenuated, and burst activity in the same neuron was replaced with irregular, single-spike activity. This neuron eventually became quiescent after prolonged depression of cortical activity. The neuron did not burst again until cortical SWA had recovered. *C*, During urethane anesthesia, GP neurons displayed a highly regular, single-spike firing pattern that was persistent during episodes of robust slow-wave activity. The GP neuron in *C* had a mean firing rate of 23.7 Hz, which is similar to the dominant frequency of activity in the Lomb, thus confirming the regular, tonic nature of its spiking. Calibration bars apply to all panels.

(mean difference of 0.07 ± 0.09 Hz), but burst-firing was phase-locked to the active or inactive components of the SWA (Fig. 8*A*). Thus, the phase relationships of firing between pairs of GPneurons were highly variable, with differences in neuronal spike timing of between 50 and 330 msec (~9–177° shifts). Correlated firing of pairs of GP neurons was evident as broad peaks in the cross-correlograms; discharge was almost inversely correlated in

→

were associated with a loss of correlated activity in the same neurons (under *white bar*). Correlated burst-firing swiftly resumed when robust SWA was restored. *C*, Later in the same recording session, SWA effectively collapsed for ~40 sec, and periodicity and correlation were lost in the pair. Note that the GP neuron fired faster during the prolonged loss of SWA in *C* as compared with the short-lived loss of SWA in *B*. In this and the following figures, *CC* designates cross-correlograms of spiking activity between pairs of neurons (bin size 10 msec). Calibration bars apply to all panels.

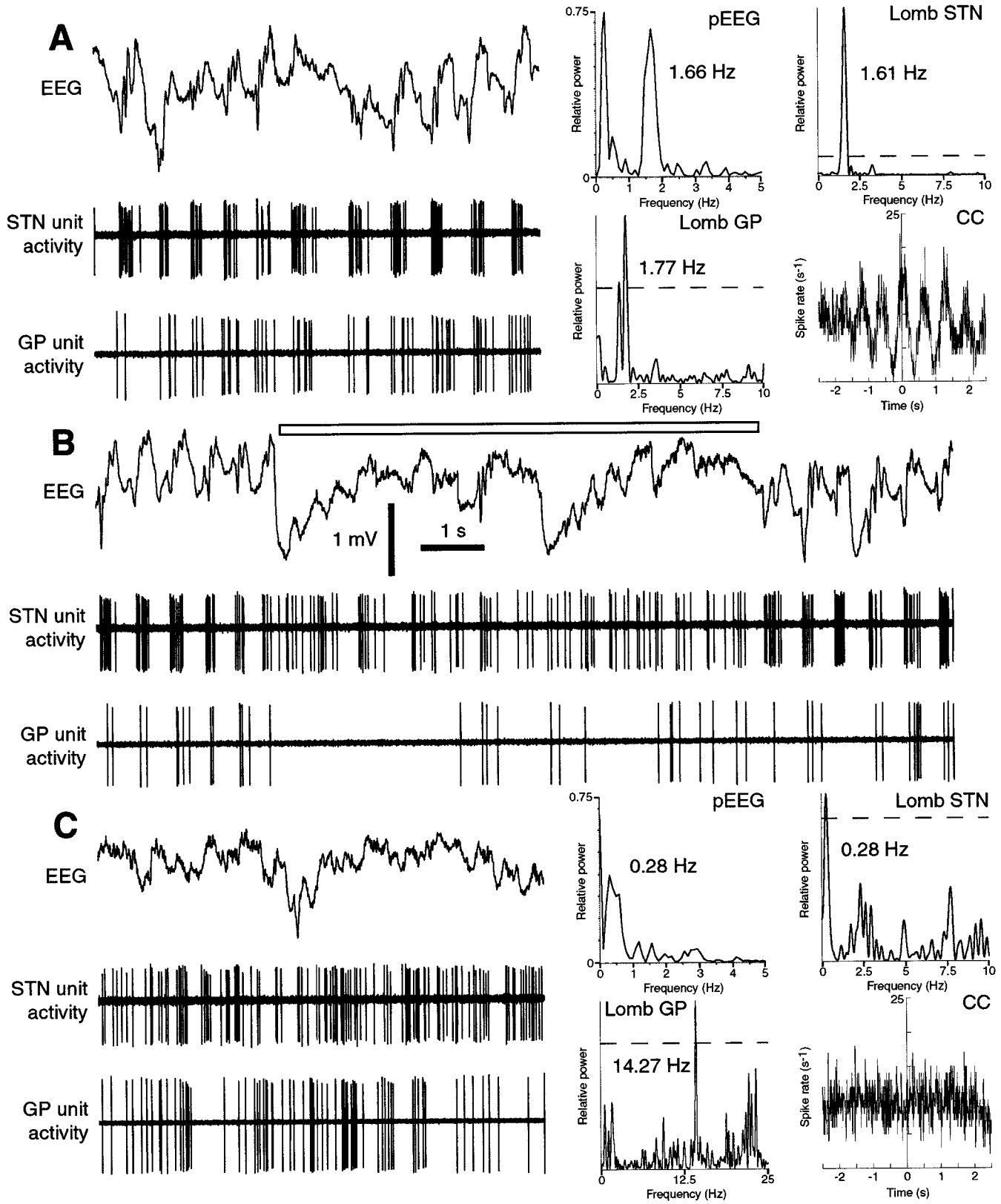

Figure 5. Simultaneous recordings of a subthalamic nucleus neuron and a globus pallidus neuron during ketamine anesthesia. *A*, This pair of bursty neurons displayed near synchronous bursting during robust SWA. Burst indices of the STN and GP neurons were 1.43 and 0.50, respectively. Burst firing of both neurons was phase-locked to the slow cortical oscillation. The cross-correlogram (*CC*) possessed several broad peaks: on average, the STN neuron fired ~30 msec before the GP neuron (18° phase difference). Narrow peaks on the millisecond time scale were not observed, which implies that the pair were not monosynaptically connected. *B*, Spontaneous, brief periods of reduction of slow-wave amplitude and rhythmicity (*Figure legend continues*)

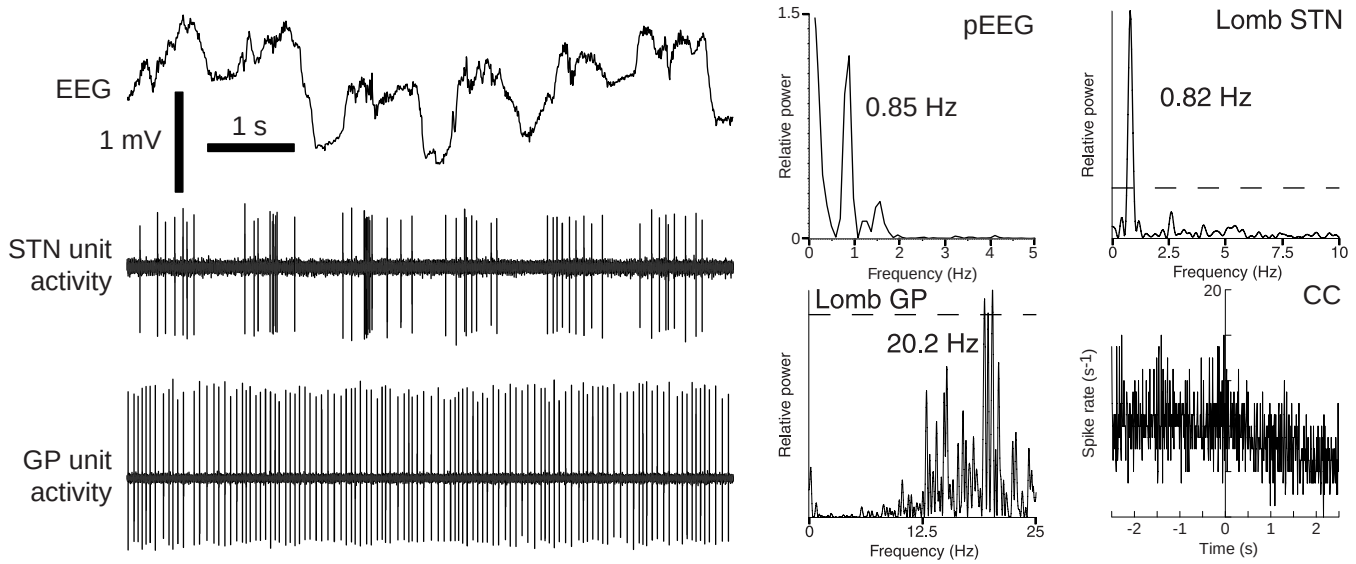

Figure 6. Simultaneous recordings of a subthalamic nucleus neuron and a globus pallidus neuron during urethane anesthesia. *A*, Typical example of uncorrelated firing in the STN–GP network. Although STN neurons fired bursts of spikes in a discrete, phase-locked manner, all GP neurons maintained a regular firing mode under this anesthetic regimen.

four pairs (Fig. 8*A*) and tended toward synchrony in two pairs (Fig. 8*B*).

To investigate the spatial aspects of network activity in the GP, the separation of pairs of GP neurons along the mediolateral axis was measured. The four inversely correlated pairs of neurons were separated by ~30, 60, 120, and 240 μm. The two pairs that tended to fire synchronously were separated by ~300 and 350 μm in the mediolateral axis. Although these data imply that neurons tending toward synchronous firing are more distantly placed and that more closely placed cells are inversely correlated, this sample is not large enough to allow firm conclusions to be made about the possible association between the position and firing relationships of GP neuron pairs.

Attenuation of SWA was associated with a loss of correlated firing (Fig. 8*C*). Thus, correlated activity in the GP depended on the direct and/or indirect influences of the cortex.

DISCUSSION

The results of this study demonstrate directly that the spike discharge properties of neurons in the STN–GP network are strictly related to coincidental cortical activity and hence the sleep–wake cycle. Simultaneous recordings of STN and GP neurons in ketamine anesthesia revealed that oscillatory activity was correlated with ongoing SWA and with each other. Correlated oscillatory activity was lost during cortical activation or depression, implying that rhythmic, synchronous inputs are required for the expression of this activity in the STN–GP network. Paired intranuclear recordings suggest that the continuum of phase relationships between STN and GP neurons is attributable, in part, to asynchronous activity within each parent nucleus.

Rhythmic oscillatory activity of the cerebral cortex is transmitted to the STN–GP network

The EEGs of rats anesthetized with ketamine were dominated by a slow, rhythmic oscillation with a frequency of ~1 Hz that was similar in form to that previously described in naturally sleeping or anesthetized cats and humans (Steriade et al., 1993c; Achermann and Borbély, 1997; Amzica and Steriade, 1998; Steriade and Amzica, 1998). In accordance with previous observations, this slow oscillation triggered and grouped delta (1–4 Hz) and spindle (7–14 Hz) oscillations (Contreras and Steriade, 1995, 1997a; Amzica and Steriade, 1998; Steriade and Amzica, 1998). During the slow oscillation, neuronal discharge is highly synchronized across large areas of the cortex (Adrian and Matthews, 1934; Amzica and Steriade, 1995; Destexhe et al., 1999) and is associated with rhythmic depolarizing (active component) and hyperpolarizing (inactive component) shifts in the membrane potential of principal neurons (Contreras and Steriade, 1995, 1997a). Since corticosubthalamic neurons are likely to be entrained during SWA (Evarts, 1964; Féger et al., 1994; Stern et al., 1997) and brief electrical stimulation of the cortex drives burst-firing of subthalamic neurons (Kitai and Deniau, 1981; Rouzaire-Dubois and Scarnati, 1985; Fujimoto and Kita, 1993), it is likely that rhythmic cortical activity is transmitted directly to the STN. Indeed, our data indicate that diverse oscillatory cortical activity may be simultaneously and faithfully represented in the spike trains of subthalamic neurons. Thus, STN neurons fired large bursts of spikes (of several hundred milliseconds duration) during the active components with a periodicity that closely matched the coincident cortical slow oscillation. Furthermore, these large bursts of activity were occasionally subdivided into smaller bursts of activity (<100 msec duration), the frequency of which was similar to the frequency of coincident faster activity (i.e., spindle-like events) in the EEG.

Slow and spindle oscillatory frequencies of the EEG were also reflected in the spike trains of GP neurons. The major routes of transmission of cortical information to the GP are via indirect pathways involving the STN and the striatum (Smith et al., 1998). It seems unlikely that the direct corticopallidal pathway (Naito and Kita, 1994) contributes substantially to oscillatory activity in the GP because it has been demonstrated that it is the STN that mediates the excitatory responses of GP neurons to brief electrical stimulation of the cortex (Nambu et al., 1990; Ryan and Clark, 1991; Kita, 1992; Yoshida et al., 1993; Maurice et al., 1998a). Thus, the oscillatory firing of GP neurons observed in this and

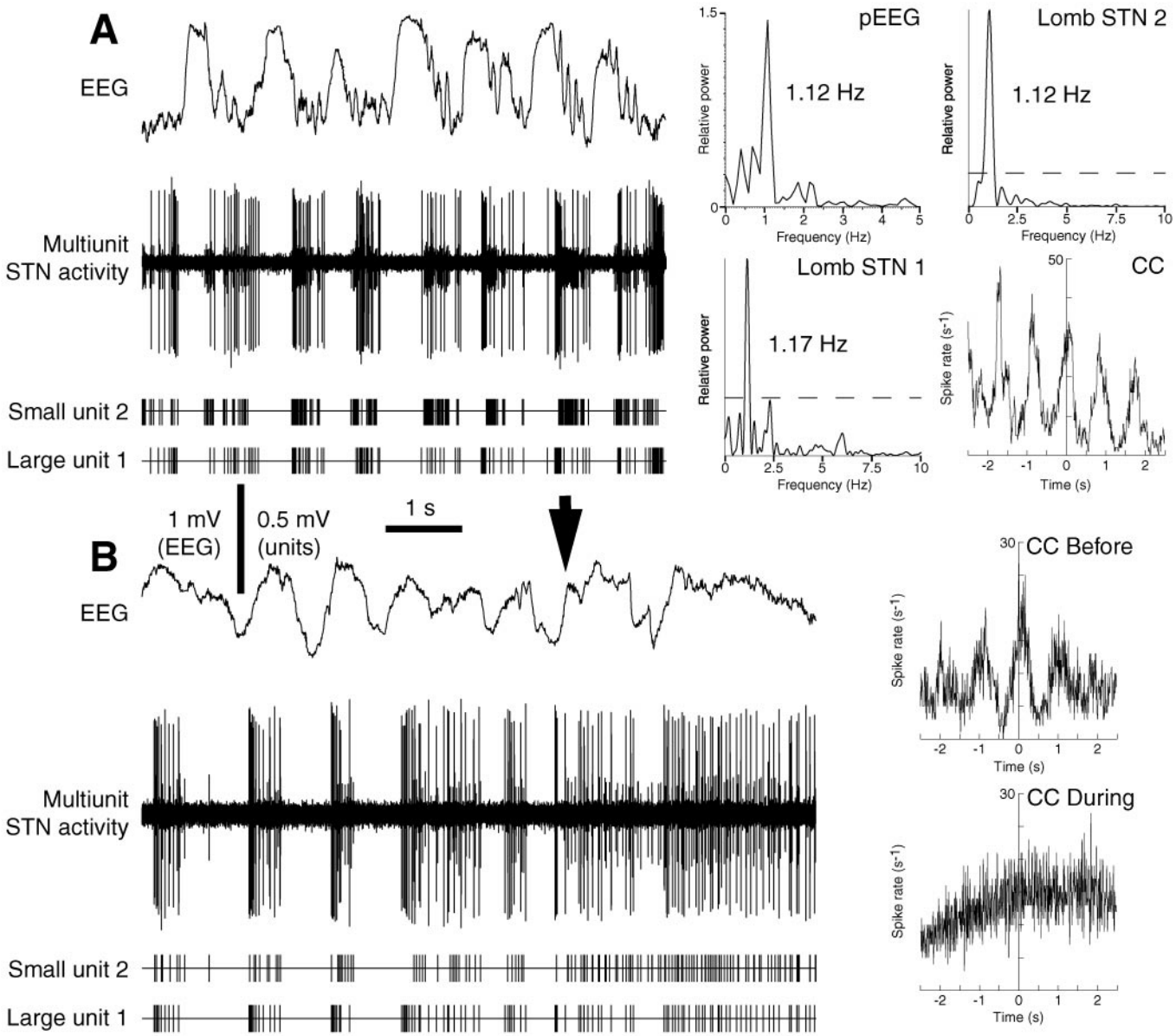

Figure 7. Near neighbors in the subthalamic nucleus exhibit synchronous, phase-locked firing during robust SWA. *A*, Multiunit recording from a single electrode during ketamine anesthesia demonstrated that the firing of STN neurons in close proximity was tightly correlated. This pair showed a small phase lag of ~30 msec (12°). The *bottom two traces* are spike-triggered digital-pulse trains dissected from the unit recordings and show more clearly the individual patterns of spike-firing of the two neurons. Both neurons had a BI of 1.43. *B*, Multiunit recordings showing near synchronous firing of neighboring STN neurons during urethane anesthesia (phase difference of ~60 msec). Disruption of the robust SWA by pinching (*black arrow*) was associated with transitions to irregular single-spike firing by the two neurons and a loss of correlated activity. Calibration bars apply to both panels.

other studies is probably a consequence of periodic excitation of the STN and subsequent feed-forward input to the GP (Morison and Bassett, 1945; Buchwald et al., 1961; Détári et al., 1987; Buzsáki, 1991; Ryan and Sanders, 1993; Nuñez, 1996; Ruskin et al., 1999). Further evidence for this is provided by our simultaneous recordings of GP and STN units during SWA, which demonstrated that oscillations in the spike trains of neurons in the two nuclei possessed very similar frequencies. In contrast to STN neurons, however, burst-firing of GP neurons was sometimes phase-locked to inactive components of the slow oscillation. Complex responses like this are difficult to interpret because of the possible involvement of trans-striatal and trans-thalamic routes of cortical information flow in shaping oscillatory activity in the STN–GP network (Ryan and Clark, 1992; Ryan et al., 1992; Maurice et al., 1998a). Indeed, the activity of striatal and thalamic inputs may also be phase-locked to cortical SWA (Steriade et al., 1990, 1993b; Stern et al., 1997, 1998).

In accordance with studies in other species, the frequency of the slow cortical oscillation was significantly slower during urethane anesthesia than during ketamine anesthesia, and STN neurons discharged in bursts of less intensity (Steriade et al., 1993c). Nevertheless, bursting was again tightly correlated with the coincident slow cortical oscillation. In contrast, all GP neurons adopted a regular firing pattern, which was unrelated to cortical SWA. A possible explanation for this is that the weaker STN activity under this anesthetic regimen is insufficient to relay the

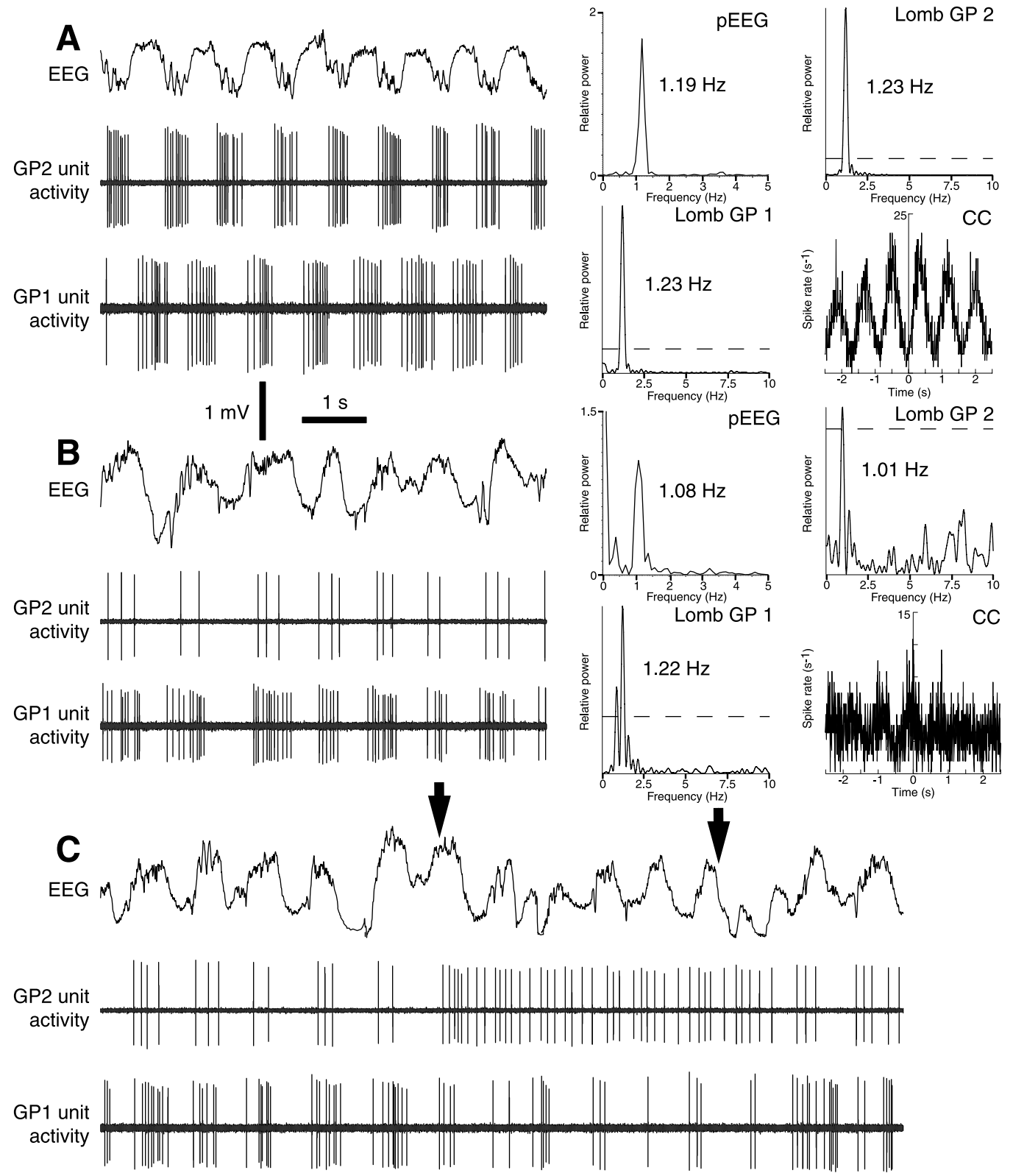

Figure 8. Simultaneous recordings of pairs of globus pallidus neurons during ketamine anesthesia. *A*, Phase-locked burst-firing in a pair of GP neurons. The neurons had an identical frequency of oscillation in their spike trains, which was similar in frequency to the cortical slow oscillation. Unit 1 (BI = 0.5) selectively fired during the inactive component of the SWA, and unit 2 (BI = 1.0) only fired during the active component. Thus, their firing was inversely correlated with a phase lag of ~400 msec (176°). *B*, The burst-firing of another pair of GP neurons was much more closely synchronized with a phase difference of ~60 msec (24°). *C*, Heterogeneous response of neurons in *B* to a 5 sec hindpaw pinch (between *black arrows*). Unit 2 adopted a regular-firing mode with a small increase in firing rate; in contrast, unit 1 maintained a burst-firing mode, but with a decreased firing rate. This diverse response resulted in uncorrelated firing between the two neurons. Calibration bars apply to all panels.

slow cortical oscillation to the GP and drive burst-firing. Indeed, during simultaneous recordings of STN and GP neurons, we observed weak burst-firing of STN neurons that was coincident with regular activity of GP neurons. Although the pairs may not have been recorded in connected regions of the network, this observation challenges the view that the STN is a driving force of neuronal activity in the basal ganglia in resting animals (Smith et al., 1998). The independent, highly regular discharge of GP neurons in this preparation implies that intrinsic pacemaker properties, which have been observed *in vitro* (Nambu and Llinás, 1994; Stanford and Cooper, 1999), may also underlie their discharge *in vivo*.

Activity of the STN–GP network is related to the sleep–wake cycle

The amplitude of the EEG is closely related to the spatial and temporal coherence of activity in cortical and thalamic neuronal networks (Contreras and Steriade, 1997a,b). Spontaneous decreases in the amplitude of SWA are the result of reductions in the synchrony of cortical principal cell firing and arise from fluctuations in the depth of anesthesia or sleep–wake state (Contreras and Steriade, 1997b). Changes of this nature in the cortex were always reflected in the activity of the STN–GP network. Sensory stimulation resulted in a similar disruption of rhythmic activity in the STN–GP network. The effects of paw pinch on the EEG were similar to those that have been reported after electrical stimulation of the midbrain reticular activating system (Moruzzi and Magoun, 1949), which suppresses the periods of hyperpolarization associated with the slow oscillation leading to increased cortical activity and a reduction in long-range cortical synchrony (Steriade et al., 1993a). Thus, the increase in GP neuronal activity during pinch may have resulted from increased cortical drive that was relayed to the GP by the STN (Ryan and Clark, 1991; Ryan and Sanders, 1993). This is in agreement with previous studies that have reported increased GP activity during the transition from sleep to waking (Détári and Vanderwolf, 1987; Détári et al., 1987; Nuñez, 1996; Chernyshev and Weinberger, 1998). The changes in firing pattern after pinch may also have been driven by the intralaminar thalamic nuclei. These nuclei are major targets of the midbrain reticular activating system (Steriade et al., 1990), send excitatory projections to the STN–GP network (Bevan et al., 1995; Mouroux et al., 1995; Smith et al., 1998), and increase their activity during painful stimuli (Peschanski et al., 1981). Taken together, these data illustrate that in our preparation, activity in the STN–GP network is intimately related to the state of activity in the cortex, and hence the sleep–wake cycle, and that rhythmic burst activity is dependent on coincident cortical oscillations.

Temporal and spatial relationships of STN–GP network activity

Rhythmic neuronal activity in the STN–GP network was correlated during SWA with periodicity similar to the slow cortical oscillation. However, the phase relationships of firing of neurons within the STN or GP and between the nuclei were variable. The phase differences of intranuclear GP recordings were greater than those from within the STN. Our intranuclear recordings from the STN and GP are in contrast to observations made in the cortex and the striatum during SWA, in which it has been shown that activity is synchronous across wide areas (Buzsáki et al., 1988; Amzica and Steriade, 1995; Contreras and Steriade, 1997a; Stern et al., 1997, 1998; Destexhe et al., 1999). It is likely that the disparate phase relationships within the STN and GP contributed to the variable phase relationships between the nuclei. These phase differences might also be generated within the STN–GP network by open and closed subthalamopallidal loops (Smith et al., 1990; Ryan and Clark, 1991; Shink et al., 1996; Bevan et al., 1997; Joel and Weiner, 1997) and/or by local intranuclear connectivity (Kita et al., 1983a; Kita and Kitai, 1994; Bevan et al., 1998; Huntsman et al., 1999). Even when pairs of neurons displayed synchronous burst activity, correlations on the low millisecond time scale, which might indicate shared synaptic input or monosynaptic relationships, were not observed (Bergman and DeLong, 1989; Ryan et al., 1992; Wichmann et al., 1994). During SWA, cortical regions may oscillate with small phase lags (Buzsáki et al., 1988). Lags in cortical afferent activity therefore are likely to contribute to the continuum of phase relationships seen in the network. Taken together, these data indicate that the firing pattern and periodicity of STN and GP neurons is dependent on coincident cortical activity, but the phase relationship of activities in these structures may be regulated in a complex manner in space by a pattern of connectivity that ensures a low degree of input sharing.

The cortex is the pattern generator of the STN–GP network

The effective removal of cortical influence on the STN–GP network by spreading depression caused an immediate loss of burst activity and a reduction in firing rates. Burst activity only resumed after recovery of SWA. Thus, the STN–GP network did not support oscillatory activity after the removal of oscillatory cortical input. This finding is in contrast to the thalamus, which contains similar ensembles of reciprocally connected excitatory and inhibitory neurons that can generate and sustain spindle oscillations in the absence of cortical influence (Morison and Bassett, 1945; Contreras et al., 1996, 1997; McCormick and Bal, 1997). It is thus likely that the cortex is primarily responsible for spindle-related bursting in the STN–GP network because if thalamic inputs were dominant, then the bursting would be evident even when the cortex was inactivated.

Functional considerations

Recent EEG studies have suggested a role for low-frequency oscillations (<3 Hz) in the preparation and execution of motor commands (Gevins et al., 1989; Bringmann, 1995; McAuley et al., 1999). The function of low-frequency oscillatory activity in cortical–basal ganglia–thalamocortical loops during sleep is unknown, but it may help to consolidate motor programs established during wakefulness (Steriade, 1999). The shift in the activity of the STN–GP network during the transition from sleep to waking is similar to that reported in other forebrain regions and is likely to reflect more efficient information processing (Détári and Vanderwolf, 1987; Buzsáki et al., 1988; Steriade et al., 1990, 1993a; Nuñez, 1996). The failure of the STN–GP network to support low-frequency oscillations when isolated from the cortex suggests that oscillations observed in this network and its targets in Parkinson's disease are derived from tremor-related activity of corticofugal systems. We cannot exclude the possibility, however, that when dopaminergic tone is reduced, the STN–GP network itself can develop tremorgenic activity (Hassani et al., 1996; Kreiss et al., 1997; Plenz et al., 1997; Bergman et al., 1998). However, any emergent oscillatory activity in the STN–GP network is still likely to be influenced by descending cortical input (Contreras and Steriade, 1997a; Contreras et al., 1996, 1997).

REFERENCES

Abeles M (1982) Quantification, smoothing, and confidence limits for single-units' histograms. J Neurosci Methods 5:317–325.

Achermann P, Borbély AA (1997) Low-frequency (<1 Hz) oscillations in the human sleep electroencephalogram. Neuroscience 81:213–222.

Adrian ED, Matthews BHC (1934) The interpretation of potential waves in the cortex. J Physiol (Lond) 81:440–471.

Albe-Fessard D, Condes-Lara M, Kesar S, Sanderson P (1983) Tonic cortical controls acting on spontaneous and evoked thalamic activity. In: Somatosensory integration in the thalamus (Macchi G, Rustioni A, Spreafico R, eds), pp 273–285. Amsterdam: Elsevier.

Aldridge JW, Gilman S (1991) The temporal structure of spike trains in the primate basal ganglia: afferent regulation of bursting demonstrated with precentral cerebral cortical ablation. Brain Res 543:123–138.

Aldridge JW, Gilman S, Dauth G (1990) Spontaneous neuronal unit activity in the primate basal ganglia and the effects of precentral cerebral cortical ablations. Brain Res 516:46–56.

Alexander GE, Crutcher MD (1990) Functional architecture of basal ganglia circuits: neural substrates of parallel processing. Trends Neurosci 13:266–271.

Amzica F, Steriade M (1995) Short- and long-range neuronal synchronization of the slow (<1 Hz) cortical oscillation. J Neurophysiol 73:20–37.

Amzica F, Steriade M (1998) Cellular substrate and laminar profile of sleep K-complex. Neuroscience 82:671–686.

Angel A, Gratton DA (1982) The effect of anesthetic agents on cerebral cortical responses in the rat. Br J Pharmacol 76:541–549.

Armstrong-James M, Fox K (1983) Similarities in unitary cortical activity between slow-wave sleep and light urethane anaesthesia in the rat. J Physiol (Lond) 346:55P.

Bergman H, DeLong MR (1989) Electro-physiological studies of the connections between the subthalamic nucleus (STN) and globus pallidus (GP) in behaving monkeys. Soc Neurosci Abstr 15:902.

Bergman H, Wichmann T, Karmon B, DeLong MR (1994) The primate subthalamic nucleus. II. Neuronal activity in the MPTP model of Parkinsonism. J Neurophysiol 72:507–520.

Bergman H, Feingold A, Nini A, Raz A, Slovin H, Abeles M, Vaadia E (1998) Physiological aspects of information processing in the basal ganglia of normal and parkinsonian primates. Trends Neurosci 21:32–38.

Bevan MD, Francis CF, Bolam JP (1995) The glutamate-enriched cortical and thalamic input to neurons in the subthalamic nucleus of the rat. J Comp Neurol 361:491–511.

Bevan MD, Clarke NP, Bolam JP (1997) Synaptic integration of functionally diverse pallidal information in the entopeduncular nucleus and subthalamic nucleus in the rat. J Neurosci 17:308–324.

Bevan MD, Booth PAC, Eaton SA, Bolam JP (1998) Selective innervation of neostriatal interneurons by a subclass of neuron in the globus pallidus of the rat. J Neurosci 18:9438–9452.

Bolam JP (Ed) (1992) Experimental neuroanatomy. Oxford, UK: Oxford UP.

Boraud T, Bezard E, Guehl D, Bioulac B, Gross C (1998) Effects of L-DOPA on neuronal activity of the globus pallidus externalis (GPe) and globus pallidus internalis (GPi) in the MPTP-treated monkey. Brain Res 787:157–160.

Bringmann A (1995) Different functions of rat's pedunculopontine tegmental nucleus are reflected in cortical EEG. NeuroReport 6:2065–2068.

Buchwald NA, Wyers EJ, Okuma T, Heuser G (1961) The "caudate-spindle." I. Electrophysiological properties. Electroencephalogr Clin Neurophysiol 13:509–518.

Buzsáki G (1991) The thalamic clock: emergent network properties. Neuroscience 41:351–364.

Buzsáki G, Bickford RG, Ponomareff G, Thal LJ, Mandel R, Gage FH (1988) Nucleus basalis and thalamic control of neocortical activity in the freely moving rat. J Neurosci 8:4007–4026.

Canteras NS, Shammah-Lagnado SJ, Silva BA, Ricardo JA (1990) Afferent connections to the subthalamic nucleus; a combined retrograde and anterograde horseradish peroxidase study in the rat. Brain Res 513:43–59.

Chernyshev BV, Weinberger NM (1998) Acoustic frequency tuning of neurons in the basal forebrain of the waking guinea pig. Brain Res 793:79–94.

Contreras D, Steriade M (1995) Cellular basis of EEG slow rhythms: a study of dynamic corticothalamic relationships. J Neurosci 15:604–622.

Contreras D, Steriade M (1997a) Synchronization of low-frequency rhythms in corticothalamic networks. Neuroscience 76:11–24.

Contreras D, Steriade M (1997b) State-dependent fluctuations of low-frequency rhythms in corticothalamic networks. Neuroscience 76:25–38.

Contreras D, Destexhe A, Sejnowski TJ, Steriade M (1996) Control of spatiotemporal coherence of a thalamic oscillation by corticothalamic feedback. Science 274:771–774.

Contreras D, Destexhe A, Steriade M (1997) Spindle oscillations during cortical spreading depression in naturally sleeping cats. Neuroscience 77:933–936.

Destexhe A, Contreras D, Steriade M (1999) Spatiotemporal analysis of local field potentials and unit discharges in cat cerebral cortex during natural wake and sleep states. J Neurosci 19:4595–4608.

Détári L, Vanderwolf CH (1987) Activity of identified cortically projecting and other basal forebrain neurones during large slow waves and cortical activation in anaesthetized rats. Brain Res 437:1–8.

Détári L, Juhasz G, Kukorelli T (1987) Neuronal firing in the pallidal region: firing patterns during sleep-wakefulness cycle in cats. Electroencephalogr Clin Neurophysiol 67:159–166.

Evarts EV (1964) Temporal patterns of discharge of pyramidal tract neurons during sleep and waking in the monkey. J Neurophysiol 27:152–171.

Féger J, Bevan MD, Crossman AR (1994) The projections from the parafascicular thalamic nucleus to the subthalamic nucleus and the striatum arise from separate neuronal populations: a comparison with the corticostriatal and corticosubthalamic efferents in a retrograde fluorescent double-labeling study. Neuroscience 60:125–132.

Filion M, Tremblay, L (1991) Abnormal spontaneous activity of globus pallidus neurons in monkeys with MPTP-induced parkinsonism. Brain Res 547:142–151.

Fujimoto K, Kita H (1992) Response of rat substantia nigra *pars reticulata* units to cortical stimulation. Brain Res 142:105–109.

Fujimoto K, Kita H (1993) Response characteristics of subthalamic neurons to the stimulation of the sensorimotor cortex in the rat. Brain Res 609:185–192.

Gevins AS, Cutillo BA, Bressler SL, Morgan NH, White RM, Illes J, Greer DS (1989) Event-related covariances during a bimanual visuomotor task. II. Preparation and feedback. Electroencephalogr Clin Neurophysiol 74:147–160.

Hassani OK, Mouroux M, Féger J (1996) Increased subthalamic neuronal activity after nigral dopaminergic lesion independent of disinhibition via the globus pallidus. Neuroscience 72:105–115.

Horikawa K, Armstrong WE (1988) A versatile means of intracellular labeling: injection of biocytin and its detection with avidin conjugates. J Neurosci Methods 25:1–11.

Horikawa K, Armstrong WE (1991) A biocytin-containing compound *N*-(2-aminoethyl)biotinamide for intracellular labeling and neuronal tracing studies: comparison with biocytin. J Neurosci Methods 37:141–150.

Huntsman MM, Porcello DM, Homanics GE, DeLorey TM, Huguenard JR (1999) Reciprocal inhibitory connections and network synchrony in the mammalian thalamus. Science 283:541–543.

Joel D, Weiner I (1997) The connections of the primate subthalamic nucleus: indirect pathways and the open-interconnected scheme of basal ganglia-thalamocortical circuitry. Brain Res Rev 23:62–78.

Kaneoke Y, Vitek JL (1996) Burst and oscillation as disparate neuronal properties. J Neurosci Methods 68:221–223.

Kita H (1992) Responses of globus pallidus neurons to cortical stimulation: intracellular study in the rat. Brain Res 589:84–90.

Kita H, Kitai ST (1994) The morphology of globus pallidus projection neurons in the rat: an intracellular staining study. Brain Res 636:308–319.

Kita H, Chang HT, Kitai ST (1983a) The morphology of intracellularly labeled rat subthalamic neurons: a light microscopic analysis. J Comp Neurol 215:245–257.

Kita H, Chang HT, Kitai ST (1983b) Pallidal inputs to subthalamus: intracellular analysis. Brain Res 264:255–265.

Kitai ST, Deniau JM (1981) Cortical inputs to the subthalamus: intracellular analysis. Brain Res 214:411–415.

Kreiss DS, Mastropietro CW, Rawji SS, Walters JR (1997) The responses of subthalamic nucleus neurons to dopamine receptor stimulation in a rodent model of Parkinson's disease. J Neurosci 17:6807–6819.

Leão AAP (1944) Spreading depression of activity in the cerebral cortex. J Neurophysiol 7:359–390.

Maggi CA, Melli A (1986) Suitability of urethane anaesthesia for phys-

iopharmacological investigations in various systems. Part 1: General considerations. Experientia 42:109–210.
Maurice N, Deniau JM, Glowinski J, Thierry AM (1998a) Relationships between the prefrontal cortex and the basal ganglia in the rat: physiology of the corticosubthalamic circuits. J Neurosci 18:9539–9546.
Maurice N, Deniau JM, Menetrey A, Glowinski J, Thierry AM (1998b) Prefrontal cortex-basal ganglia circuits in the rat: involvement of ventral pallidum and subthalamic nucleus. Synapse 29:363–370.
Maurice N, Deniau JM, Glowinski J, Thierry AM (1999) Relationships between the prefrontal cortex and the basal ganglia in the rat: physiology of the cortico-nigral circuits. J Neurosci 19:4674–4681.
McAuley JH, Framer SF, Rithwell JC, Marsden CD (1999) Common 3 Hz and 10 Hz oscillations modulate human eye and finger movements while they simultaneously track a visual target. J Physiol (Lond) 515:905–917.
McCormick DA, Bal T (1997) Sleep and arousal: thalamocortical mechanisms. Annu Rev Neurosci 20:185–215.
Metherate R, Cox CL, Ashe JH (1992) Cellular bases of neocortical activation: modulation of neural oscillations by the nucleus basalis and endogenous acetylcholine. J Neurosci 12:4701–4711.
Morison RS, Bassett DL (1945) Electrical activity of the thalamus and basal ganglia in decorticate cats. J Neurophysiol 8:309–314.
Moruzzi G, Magoun HW (1949) Brain stem reticular formation and activation of the EEG. Electroencephalogr Clin Neurophysiol 1:455–473.
Mouroux M, Hassani OK, Féger J (1995) Electrophysiological study of the excitatory parafascicular projection to the subthalamic nucleus and evidence for ipsi- and contralateral controls. Neuroscience 67:399–407.
Naito A, Kita H (1994) The cortico-pallidal projection in the rat: an anterograde tracing study with biotinylated dextran amine. Brain Res 653:251–257.
Nambu A, Llinás RR (1994) Electrophysiology of globus pallidus neurons in vitro. J Neurophysiol 72:1127–1139.
Nambu A, Yoshida SI, Jinnai K (1990) Discharge patterns of pallidal neurons with input from various cortical areas during movement in the monkey. Brain Res 519:183–191.
Nini A, Feingold A, Slovin H, Bergman H (1995) Neurons in the globus pallidus do not show correlated activity in the normal monkey, but phase-locked oscillations appear in the MPTP model of Parkinsonism. J Neurophysiol 74:1800–1805.
Nuñez A (1996) Unit activity of rat basal forebrain neurons: relationship to cortical activity. Neuroscience 72:757–766.
Paxinos G, Watson C (1986) The rat brain in stereotaxic coordinates, Ed 2. Sydney: Academic.
Perkel DH, Gerstein GL, Moore GP (1967) Neuronal spike trains and stochastic point processes. II. Simultaneous spike trains. Biophys J 7:419–440.
Peschanski M, Guilbaud G, Gautron M (1981) Posterior intralaminar region in rat: neuronal responses to noxious and non-noxious cutaneous stimuli. Exp Neurol 72:226–238.
Pinault D (1996) A novel single-cell staining procedure performed *in vivo* under electrophysiological control: morpho-functional features of juxtacellularly labeled thalamic cells and other central neurons with biocytin or Neurobiotin. J Neurosci Methods 65:113–136.
Plenz D, Herrera-Marschitz M, Kitai ST (1997) The oscillatory feedback circuitry between subthalamic nucleus and globus pallidus as a putative generator for resting tremor. Soc Neurosci Abstr 23:463.
Robledo P, Féger J (1990) Excitatory influence of rat subthalamic nucleus to substantia nigra *pars reticulata* and the pallidal complex: electrophysiological data. Brain Res 518:47–54.
Rouzaire-Dubois B, Scarnati E (1985) Bilateral corticosubthalamic nucleus projections: electrophysiological study in rats with chronic cerebral lesions. Neuroscience 15:69–79.
Rouzaire-Dubois B, Scarnati E (1987) Pharmacological study of the cortical-induced excitation of subthalamic neurons in the rat: evidence for amino acids as putative neurotransmitters. Neuroscience 21:429–440.
Rouzaire-Dubois B, Hammond C, Hamon B, Féger J (1980) Pharmacological blockade of the globus pallidus-induced inhibitory response of subthalamic cells in the rat. Brain Res 200:321–329.
Ruskin DN, Bergstrom DA, Kaneoke Y, Patel BN, Twery MJ, Walters JR (1999) Multisecond oscillations in firing rate in the basal ganglia: robust modulation by dopamine receptor activation and anesthesia. J Neurophysiol 81:2046–2055.
Ryan LJ, Clark KB (1991) The role of the subthalamic nucleus in the response of globus pallidus neurons to stimulation of the prelimbic and agranular frontal cortices in rats. Exp Brain Res 86:641–651.
Ryan LJ, Clark KB (1992) Alteration of neuronal responses in the subthalamic nucleus following globus pallidus and neostriatal lesions in rats. Brain Res Bull 29:319–327.
Ryan LJ, Sanders DJ (1993) Subthalamic nucleus lesion regularizes firing patterns in globus pallidus and substantia nigra pars reticulata neurons in rats. Brain Res 626:327–331.
Ryan LJ, Sanders DJ (1994) Subthalamic nucleus and globus pallidus lesions alter activity in nigrothalamic neurons in rats. Brain Res Bull 34:19–26.
Ryan LJ, Sanders DJ, Clark KB (1992) Auto- and cross-correlation analysis of subthalamic nucleus neuronal activity in neostriatal- and globus pallidal-lesioned rats. Brain Res 583:253–261.
Shink E, Bevan MD, Bolam JP, Smith Y (1996) The subthalamic nucleus and the external pallidum: two tightly interconnected structures that control the output of the basal ganglia in the monkey. Neuroscience 73:335–357.
Smith Y, Bolam JP, von Krosigk M (1990) Topographical and synaptic organization of the GABA-containing pallidosubthalamic projection in the rat. Eur J Neurosci 2:500–511.
Smith Y, Bevan MD, Shink E, Bolam JP (1998) Microcircuitry of the direct and indirect pathways of the basal ganglia. Neuroscience 86:353–387.
Stanford IM, Cooper AJ (1999) Presynaptic μ and δ opioid receptor modulation of GABAa IPSCs in the rat globus pallidus *in vitro*. J Neurosci 19:4796–4803.
Steriade M (1999) Coherent oscillations and short-term plasticity in corticothalamic networks. Trends Neurosci 22:337–345.
Steriade M, Amzica F (1998) Coalescence of sleep rhythms and their chronology in corticothalamic networks. Sleep Res Online 1:1–10.
Steriade M, Jones EG, Llinás RR (1990) Thalamic oscillations and signaling. New York: Wiley-Interscience.
Steriade M, Amzica F, Nuñez A (1993a) Cholinergic and noradrenergic modulation of the slow ($\approx$ 0.3 Hz) oscillation in neocortical cells. J Neurophysiol 70:1385–1400.
Steriade M, Contreras D, Curró Dossi R, Nuñez A (1993b) The slow ($<$1 Hz) oscillation in reticular thalamic and thalamocortical neurons: scenario of sleep rhythm generation in interacting thalamic and neocortical networks. J Neurosci 13:3284–3299.
Steriade M, Nuñez A, Amzica F (1993c) A novel slow ($<$1 Hz) oscillation of neocortical neurons *in vivo*: depolarizing and hyperpolarizing components. J Neurosci 13:3252–3265.
Steriade M, Nuñez A, Amzica F (1993d) Intracellular analysis of relations between the slow ($<$1 Hz) neocortical oscillation and other sleep rhythms of the electroencephalogram. J Neurosci 13:3266–3283.
Stern EA, Kincaid AE, Wilson CJ (1997) Spontaneous subthreshold membrane potential fluctuations and action potential variability of rat corticostriatal and striatal neurons *in vivo*. J Neurophysiol 77:1697–1715.
Stern EA, Jaeger D, Wilson CJ (1998) Membrane potential synchrony of simultaneously recorded striatal spiny neurons *in vivo*. Nature 394:475–478.
Svoboda K, Helmchen F, Denk W, Tank D (1999) Spread of dendritic excitation in layer 2/3 pyramidal neurons in rat barrel cortex *in vivo*. Nature Neurosci 2:65–73.
Wichmann T, Bergman H, DeLong MR (1994) The primate subthalamic nucleus. I. Functional properties in intact animals. J Neurophysiol 72:494–506.
Yoshida S, Nambu A, Jinnai K (1993) The distribution of the globus pallidus neurons with input from various cortical areas in the monkey. Brain Res 611:170–174.